Diminished Adherence of Biomphalaria Glabrata Embryonic Cell Line to Sporocysts of Schistosoma Mansoni Following Programmed Knockout of the Allograft Inflammatory Factor

Fernanda Sales Coelho
Grupo de PesquisaemHelmintologia e MalacologiaMédica, Instituto René Rachou, Fundação Oswaldo Cruz, Belo Horizonte, MG, Brazil.

Rutchanee Rodpai
Department of Microbiology, Immunology and Tropical Medicine, School of Medicine and Health Sciences, George Washington University, Washington, D.C., USA

Andre Miller
Biomedical Research Institute , Schistosomiasis Resource Center, Rockville, MD, USA

Shannon E Karinshak
Department of Microbiology, Immunology and Tropical Medicine, School of Medicine and Health Sciences, George Washington University, Washington, D.C., USA

Victoria H Mann
Department of Microbiology, Immunology and Tropical Medicine, School of Medicine and Health Sciences, George Washington University, Washington, D.C., USA

Omar dos Santos Carvalho
Grupo de PesquisaemHelmintologia e MalacologiaMédica, Instituto René Rachou, Fundação Oswaldo Cruz, Belo Horizonte, MG, Brazil.

Roberta Lima Cladeira
Grupo de PesquisaemHelmintologia e MalacologiaMédica, Instituto René Rachou, Fundação Oswaldo Cruz, Belo Horizonte, MG, Brazil.

Marina de Moraes Mourao
Grupo de Pesquisa em Helmintologia e Malacologia Medica

Paul J Brindley
Department of Microbiology, Immunology and Tropical Medicine, School of Medicine and Health Sciences, George Washington University, Washington, D.C., USA

Wannaporn Ittiprasert (wannaporni@gwu.edu)
Department of Microbiology, Immunology and Tropical Medicine, School of Medicine and Health Sciences, George Washington University, Washington, D.C., USA https://orcid.org/0000-0001-9411-8883

Research

Keywords: Biomphalaria glabrata embryonic cell line, Bge, CRISPR/Cas9, gene editing, allograft inflammatory factor, cell adhesion

Posted Date: August 5th, 2020

DOI: https://doi.org/10.21203/rs.3.rs-51130/v1

Version of Record: A version of this preprint was published on October 13th, 2020. See the published version at https://doi.org/10.1186/s13071-020-04384-9.

Abstract

The development of the larval stage of *Schistosoma mansoni* in an intermediate host snail of the genus *Biomphalaria* is an obligatory component of the life cycle. Enhanced understanding of the mechanism(s) of host defense in the snail may hasten the development of tools that block transmission of schistosomiasis. The *B. glabrata* embryonic cell line, termed the Bge line, is a versatile resource for investigation of the snail-schistosome relationship. A key attribute of the Bge cell is the hemocyte-like phenotype, given the central role of the snail hemocyte in innate and cellular immunity. The allograft inflammatory factor 1, AIF, is evolutionarily conserved, typically is expressed in phagocytes and granular leukocytes, is a marker of macrophage activation in mammals and in invertebrates, and enhances cell proliferation and migration. AIF is highly expressed in strains of *B. glabrata* resistant *S. mansoni* infection in comparison with susceptible strains of the snail. We hypothesized that *Bg*AIF may play a role in hemocyte proliferation, adhesion and/or migration after exposure of the snail to schistosomes. CRISPR/Cas gene knockout of the *Bg*AIF gene in Bge cells was undertaken to investigate the hypothesis. Gene knockout manipulation induced gene-disrupting indels, frequently 1–2 bp insertions and/or 8–30 bp deletions, at the programmed target site; a range from 9 to 17% of *Bg*AIF genes were mutated during 12 replicate experiments, and transcript levels for *Bg*AIF were significantly reduced by up to 73% (range, 26 to 73%, mean 49.5 ± 20.2% S.D, n = 12) when monitored for up to nine days following the gene-editing manipulation. The adherence to sporocyst of *BgAIF* gene-edited (Δ*Bg*AIF) Bge cells was significantly diminished in comparison to wild type cells, even though cell morphology did not differ between Δ*Bg*AIF treatment and control groups of Bge cells. A Bge cell adherence index (CAI) to individual sporocysts was observed at 2.66 ± 0.10 for control and 2.30 ± 0.22 in Δ*Bg*AIF cells ($P < 0.05$), revealing that Δ*Bg*AIF cells were significantly less adherent than wild type Bge cells to primary sporocysts. The findings supported the hypothesis that *Bg*AIF plays a role in the adherence of *B. glabrata* hemocytes to sporocysts during schistosome infection.

Introduction

Evolution endowed the schistosomes with a complex developmental cycle, which includes both a freshwater gastropod intermediate host and a definitive mammalian host. Several species of the freshwater snail genus *Biomphalaria* are the intermediate host for *Schistosoma mansoni*. The neotropical species *Biomphalaria glabrata* has been investigated extensively with respect to host-parasite relationship and coevolution with *S. mansoni* especially on mechanisms of susceptibility and/or resistance to the compatible parasites [1, 2]. Genetic variation is evident among isolates and strains of *B. glabrata*, both in the laboratory and in the field, resulting in a spectrum of the susceptibility of infection with *S. mansoni* [3]. Considerable advances have been made in the exploration and characterization of mechanisms of the internal defenses of the snail that determine susceptibility and resistance to schistosome [4–11]. The resistance phenotype is underpinned by a complex genetic trait, where the schistosome larva fails to develop as the consequence of innate and cellular immune responses. Hemocytes of resistant snails encapsulate and destroy the sporocyst [11–18].

The *B. glabrata* embryonic cell line (Bge) [19] remains to date the only established cell line from any mollusk. The cell line originates from five-day-old embryos of *B. glabrata* susceptible to infection with *S. mansoni*. The Bge cell line has been studied extensively to interrogate the host-parasite relationship because the Bge cell exhibits a hemocyte-like behavior that includes encapsulation of the larval parasite [20–28]. The genome sequence of *B. glabrata* has been reported [29], along with ongoing transcriptome and proteome catalogues that include factors participating in immunological surveillance, phagocytosis, cytokine responses, and pathogen recognition receptor elements including Toll-like receptors and fibrinogen-related proteins [30–36]. An orthologue of the evolutionary conserved allograft inflammatory factor (AIF), which is a conserved protein typically expressed in phagocytes and granular leukocytes in both vertebrate and invertebrate. Functions demonstrated for AIF include macrophage activation, enhancement of cellular proliferation and of migration in mammalian and invertebrate cells [37–41]. AIF also plays a key role in the protective response by *B. glabrata* to invasion by schistosomes [8, 9]. *Bg*AIF, the orthologue in *B. glabrata* is expressed in hemocytes, which participate in phagocytosis, cellular proliferation, and cellular migration. Elevated expression of *Bg*AIF is a characteristic of the resistance of *B. glabrata* to schistosome infection and is a marker of hemocyte activation [8, 9].

Expression of AIF also is seen during hemocyte activation in oysters [38, 42–44] and during hepatic inflammation during murine schistosomiasis [45, 46]. We hypothesized that *Bg*AIF was involved in cell mediated immune response(s) by *B. glabrata* through activation of hemocyte cell adhesion and/or migration after the schistosome miracidium has penetrated into the tissues of the snail. We addressed this hypothesis by using CRISPR/Cas9-based programmed genome editing to interrupt the *Bg*AIF gene of *B. glabrata* in the Bge cell line, following reports that indicated the utility of using CRISPR-based programmed gene knockout approach in other mollusks including the Pacific oyster, *Crassostrea gigas* and the slipper limpet, *Crepidula fornicata* [47–49]. As detailed below, we demonstrated the activity of programmed genome editing in Bge cells, with gene knockout at the *Bg*AIF locus.

Materials And Methods

Gene editing construct

The gene encoding the allograft inflammatory factor of *B. glabrata*, *Bg*AIF (2,226 bp; accession number BGLB005061, https://www.vectorbase.org/) includes five exons interrupted by four introns (Fig. 1a). A guide RNA (gRNA) for Cas9-catalyzed gene editing specific for the target *B. glabrata* gene locus, *Bg*AIF, was identified in the BGLB005061 sequence using the ‘CHOPCHOP’ v3 tool, https://chopchop.cbu.uib.no/, with default parameters compatible for the protospacer adjacent motif, NGG, of Cas9 from *Streptococcus pyogenes* [50–52] and screened for off-target sites against *Biomphalaria glabrata* genome [29]. Based on the guidance from the CHOPCHOP analysis, we chose the top ranked guide RNA (gRNA), AGACTTTGTTAGGATGATGC, specific for exon 4 of the AIF gene, with predicted high CRISPR/Cas9 efficiency for double-stranded cleavage in tandem with an absence of off-target activity in the genome of *B. glabrata* (Fig. 1a). A CRISPR/Cas9 vector encoding the gRNA targeting exon 4 of *Bg*AIF under the control of the mammalian U6 promoter and encoding Cas 9, with nuclear localization signals 1 and 2,

driven by the human cytomegalovirus (CMV) immediate early enhancer and promoter was assembled using the GeneArt CRISPR Nuclease Vector system (Thermo Fisher Scientific, Waltham, MA), according to the manufacturer's protocol. The construct was termed pCas-*Bg*AIFx4 (Fig. 1b). Chemically competent TOP10, *E. coli* cells (Invitrogen, Thermo Fisher Scientific) were transformed with pCas-*Bg*AIFx4 by the heat shock method and cultured on LB-agar supplemented with ampicillin at 100 µg/ml. Subsequently, plasmids recovered from several single colonies of ampicillin-resistant *E. coli* transformants were confirmed for gRNA ligation and orientation by amplicon PCR-based Sanger direct nucleotide sequence analysis using a U6 gene-specific primer to confirm the integrity of inserted gRNA sequence (Fig. 1b).

Biomphalaria glabrata **embryonic (Bge) cell line culture**

The Bge cell line was provided by the Schistosomiasis Resource Center (SRC), Biomedical Research Institute (BRI), Rockville, MD. Historically, the Bge cell line was sourced by the SRC from the American Type Culture Collection (Manassas, VA), catalog no. ATCC CRL 1494, and thereafter maintained at BRI for > 10 years. Bge cells were maintained at 26ºC in air in 'Bge medium', which is comprised of 22% (v/v) Schneider's *Drosophila* medium, 0.13% galactose, 0.45% lactalbumin hydrolysate, 0.5% (v/v) phenol red solution, 20 µg/ml gentamycin, and supplemented with 10% heat-inactivated fetal bovine serum [24, 53]. Bge cells were grown to 80% confluence before transfection by electroporation with pCas-*Bg*AIFx4. The Bge cells were free of contamination with *Mycoplasma*, as established with a PCR-based test (LookOut® Mycoplasma PCR Detection kit, Sigma-Aldrich, St. Louis, MO).

Transfection Of Bge Cells By Square Wave Electroporation

Bge cells were harvested using a cell scraper, washed twice in Bge medium, counted, and resuspended at 20,000 cell/µl in Opti-MEM medium (Sigma-Aldrich, St. Louis, MO). Two million cells were transferred into 0.2 mm path length electroporation cuvettes (BTX Harvard Apparatus, Hollister, MA) containing 6 µg pCas-*Bg*AIFx4 in ~ 100 µl Opti-MEM. The cells were subjected to electroporation using one pulse at 125 volts for 20 milliseconds, using a square wave pulse generator (ECM 830, BTX Harvard Apparatus). Immediately thereafter, the Bge cells were maintained in 12-well plates (Greiner Bio-One) at 26ºC. The mock control included Opti-MEM only for electroporation. The presence of transcripts encoding the *B. glabrata* actin (*Bg*Actin) and the Cas9 was monitored daily for nine days following transfection by electroporation (Fig. 1c).

Sequential Isolation Of Total Rna And Genomic Dna

To monitor the transfection of Bge cell by pCas9-*Bg*AIFx4, we investigated the expression of Cas9 in Bge cells by reverse transcriptase PCR (RT-PCR). Both total RNA and genomic DNA were extracted sequentially from cell pellets, as previously described [54, 55]. In brief, each sample of total RNA sample was extracted using the RNAzol® RT reagent (Molecular Research Center, Inc., Cincinnati, OH) according to the manufacturer's protocol. Subsequently, the DNA/protein pellet retained after recovery of RNA was

resuspend in DNAzol® solution (Molecular Research Center, Inc), and total DNA recovered. The samples of RNA and DNA were dissolved in nuclease-free water and concentration and purity established by spectrophotometry (Nanodrop 1000, Thermo Fisher Scientific).

Expression Of Cas9 In Bge Cells

To investigate transcription from the pCas-*Bg*AIFx4 vector following transfection of Bge cells, levels of transcribed Cas9 were investigated by semi-quantitative RT-PCR. Total RNA from the non-transfected cell, mock (Opti-MEM electroporated-) and pCas-*Bg*AIFx4 DNA electroporated-Bge cells were treated with DNase I (Ambion, Thermo Fisher Scientific) to digest any residual vector pCas-*Bg*AIFx4 DNA and contaminating genomic DNAs. The RNAs were reverse transcribed to cDNA using the First Strand cDNA Synthesis kit (New England Biolabs, Ipswich, MA). RT-PCRs specific for the actin gene of *B. glabrata, Bg*Actin was also included as positive control. The primer pairs used for the *Bg*Actin and the Cas9 coding sequences were: *Bg*Actin, actin-F: 5'- GTCTCCCACACTGTACCTATC-3', actin-R: 5'-CGGTCTGCATCTCGTTTT-3'; Cas9, Cas9-F: 5'- GAGTGAACTTCCCGCCGAAT-3' and Cas9-R: 5'-GGTCTTGACGAGACGATGCT-3' (Fig. 1b). Amplicons and molecular size standards were separated by electrophoresis through Tris-acetate-EDTA-buffered agarose 1% stained with ethidium bromide (Fig. 1c).

Analysis of programmed mutation of the allograft inflammatory factor gene of B. glabrata

Genomic DNA samples from the mock-transfected and pCas-*Bg*AIFx4-transfected cells were amplified by PCR using AIF-F and AIF-R primers that flank the CRISPR/Cas9 programmed double-stranded break (DSB) site (Fig. 1a). Amplicons were isolated using the PCR cleanup and gel extraction kit (ClonTech, Takara USA, Mountain View, CA) and the nucleotide sequence of amplicons determined by Sanger direct sequencing (GENEWIZ, South Plainfield, NJ). Chromatograms of the sequence reads from the control and experimental groups in each replicate experiment were subjected to online analysis using the TIDE algorithm, https://tide.deskgen.com/ [56, 57] and also using the Inference of CRISPR v2 Edits analysis (ICE) software, https://ice.synthego.com/#/ (Synthego Corporation, Redwood City, CA) [58]. Estimates of CRISPR efficiency, insertion-deletion (INDEL)-substitution percentages, and the nucleotide sequence of mutant alleles were obtained using both the TIDE and the ICE platforms (Fig. 2a, 2b).

Quantitative real time PCR analysis of transcription of Bg**AIF**

To evaluate the differential levels of the *Bg*AIF transcript among the groups, total RNA was extracted and treated with DNase I, as above. DNase I treated-RNA (200 ng) was reverse transcribed to cDNA, followed by quantitative RT-PCR, using the ViiA7 Real Time PCR System (Applied Biosystems, Scientific), and the SSoAdvanced Universal SYBR Green Supermix reagents (Bio-Rad), according to the manufacturer's recommendations. The following nucleotide primers were used: *Bg*AIF specific forward primer, 5'-CCTGCTTTTAACCCGACAGA-3' and reverse primer, 5'-TGAATGAAAGCTCCTCGTCA-3'. Differential *Bg*AIF gene expression were calculated after normalizing with *Bg*Actin (primers as above) and comparison with

the non-treated cells (control group). The ΔΔCt method was used to calculate the differential gene expression [59], with assistance of the GraphPad Prism 8 software (San Diego, CA) (Fig. 2c).

Schistosome Sporocysts

Miracidia of NMRI strain of *S. mansoni* were hatched from eggs that were harvested from livers of schistosome infected mice (Schistosomiasis Resource Center, Biomedical Research Institute, Rockville, MD) under axenic conditions [28], primary sporocysts were transformed from the miracidia *in vitro*, as described [26]. Briefly, miracidia were immobilized by chilling on ice for 25 min, following be pelleting using centrifugation, 500· *g* at 4 °C, 60 sec. The miracidia were washed with ice cold Chernin's balanced salt solution with 1 mg/ml of glucose and trehalose and antibiotic, 10 µl/ml of 100· penicillin/streptomycin (Thermo Fisher Scientific), termed CBSS^{+}. Approximately 5,000 miracidia per well of 24-well plate were cultured in CBSS + at 26 °C for 24 hrs, after which the sporocysts were washed remove shed ciliated epidermal plates and other debris, followed by transfer to a 1.5 ml microcentrifuge tube [26].

Sporocyst-bge Cell Binding Assay And Cell Adhesion Index (cai)

To investigate the if *Bg*AIF would affect the ability of cell adhesion to *S. mansoni* sporocyst, we co-cultured the non-transfected Bge cell or *Bg*AIF depleted- cell (Δ*Bg*AIF-Bge) with *in vitro* transformed sporocysts, then the cell adhesion index (CAI) were calculated as described [26]. CAI is a semi-quantitative method of cell adhesion to primary sporocyst using the four degree of scores ranging from one to four (low to high amount of cell adhere to parasite surface). In brief, we mixed single cell suspension of 500,000 Bge cells with 200 freshly prepared-sporocysts (total volume 200 µlof CBSS^{+}) in sterile, siliconized tubes (Bio Plas, Thomas Scientific, Swedesboro, NJ). The Bge cell-sporocyst co-culture was maintained at 26 °C for 24 hrs. Cellular morphology and adhesion of the cells the surface of the parasite was monitor and recorded using a n inverted microscope (20 × magnification on Zeiss Axio Observer A1) (Carl Zeiss LLC, White Plains, NY) after gently transferring the parasite-cell suspension to

the tissue culture plate (Greiner Bio-One). Scoring of the cell index was carried out in a blinded fashion to the investigator reading the score, > 50 sporocysts from each experimental group were counted each time, and triplicates of each treatment group were scored. Seven independent biological replicates of this CAI-based sporocyst-Bge cell binding assay were carried out. In total, > 400 sporocysts were examined from each treatment and control group. Averages for the CAI values were calculated from the cell adhesion scores ranging from 1 to 4 (examples presented in Fig. 3a) according to the formula, CAI = total binding value per number of sporocysts [26].

Results

Transcription of Cas9 nuclease in Bge cells

Total RNA was extracted from non-transfected cell (wild type; WT), mock control and pCas-*Bg*AIFx4-transfected Bge cells to assess the expression of Cas9, driven by the CMV promoter (Fig. 1b). The excess of *Bg*AIFx4 plasmid DNA and cellular genomic DNAs were eliminated by DNase I digestion, the non-DNA contaminated-RNA was proceeded for cDNA synthesis. The cDNAs from either controls or pCas-*Bg*AIFx4-transfected Bge cells were employed as the template in PCRs using two primer pairs, one specific for Cas9 and the other for *Bg*Actin, the actin gene of *B. glabrata* that served as the reference gene (Fig. 1b, c). Transcripts encoding Cas9 driven by mammalian CMV promoter in transient pCas-*Bg*AIFx4 transfected-Bge cells were detected after 24 hrs after transfection and continued to express up to 9 days. The specific amplicon of Cas9 mRNA (231 bp) were observed only pCas-BgAIFx4 transfected cells, and absent in non-transfected cells (Fig. 1c). While the control of housekeeping gene expression, actin, *Bg*Actin was observed at 214 bp amplicon in both controls and experimental samples (Fig. 1c).

Programmed mutation of Bg**AIF confirmed functional CRISPR/Cas9 activity in** B. glabrata

Genomic DNAs from WT Bge, mock-transfected and pCas-*Bg*AIFx4-transfected cells were used as the template for PCRs with a primer pair; AIF-F and AIF-R flanking the expected cleavage site by CRISPR/Cas9 materials on *Bg*AIF, exon 4 (Fig. 1a, green arrows; amplicon size, ~ 200 nt). The predicted site of the Cas9-catalyzed double-strand break (DSB) within the *Bg*AIF locus is indicated by the red arrow in Fig. 1a. The nucleotide sequence of the amplicons was determined by Sanger direct sequencing using the same primers, AIF-F and AIF-R. Both forward and reverse DNA sequencing reads were analyzed for programmed CRISPR/Cas9-catalyzed mutations using two CRISPR editing software packages, the ICE and the TIDE tools [56, 57]. Both parse the Sanger sequencing files, either one at a time or as a batch of several technical replicates from the same sample, and identify the sequences complimentary to the gRNA. The tools calculate the editing efficiency and determine the profiles of all the different types of edits (mutant alleles) and their relative abundances, in comparison with sequence reads of the control samples. From our results, we investigate the presence of deletion-insertion mutations (INDELs) in both forward and reverse direction Sanger sequence reads of each sample. The reads from the Bge cells transfected with the pCas9-*Bg*AIFx4 contained INDELs at or around the programmed CRISPR/Cas9 cleavage site. The percentage of reads that included INDELs ranged from 8.9–17.1%, in the 12 biological replicates that we

carried out (Fig. 2a, b). Notably, the mutation profile in the vicinity of the predicted DSB in *Bg*AIF was similar among these 12 replicates. The 12 experiments were undertaken independently. Commonly seen INDELs at the DSBs site as revealed by the ICE analysis included deletions of 8 to 30 bp and insertions of 1 or 2 bp (Fig. 2a). These mutations were predicted to result in frameshift mutations, consequent loss of the open reading frame, and hence and permanent knockout of *Bg*AIF in the edited Bge cell. The profile of the frequency of mutations observed in each biological replicate was used to plot the curve (Prism 8 software) presented in Fig. 2b. These findings demonstrated that programmed genome editing using CRISPR/Cas9 was active in Bge cells, and that the non-homologous end-joining (NHEJ) pathway [60] was active in *B. glabrata* for the repair of programmed double-stranded breaks, leading to targeted gene knockout.

Programmed mutation interrupted expression of Bg*AIF*

The aims of the study included the investigation of the activity or not CRISPR/Cas9 gene editing in the Bge cell line and addressing the hypothesis that AIF functions in the activation of a macrophage like phenotype by the Bge cell. Accordingly, Bge cells were transfected with a CRISPR/Cas9 encoding plasmid that expressed the gRNA under control of the human U6 promoter and Cas9 driven by the CMV promoter. The experimental approach did not include drug resistance and/or reporter gene markers in order to enrich for transfected Bge cells. However, even without enrichment of the exposed Bge cell for transfected cells, a highly statistically significant reduction in levels of *Bg*AIF transcripts was seen in the Bge transfected cell population. Expression of *Bg*AIF transcripts were assessed using RNAs from the cells at nine days post transfection. Comparison of the experimental and control groups revealed significantly reduced levels of the *Bg*AIF in the pCas-*Bg*AIFx4-transfected cells, mean 49.55±20.22%, range 28.1–86.3% (n = 12) compared to the WT Bge (normalized sample, 100% expression), mock control cells (unpaired *t*-test, t = 8.584, df = 22, $P \leq 0.05$) (Fig. 1b). An inverse correlation between the percentage of INDELs and reduction in transcript levels was not apparent (not shown).

Programmed knockout of Bg*AIF* interfered with adherence of Bge cells to schistosome sporocysts

Single cell suspensions of Bge cells in the mock-treated and Δ*Bg*AIF groups were co-cultured in siliconized tubes with primary *S. mansoni* sporocysts for 24 hrs. At that point, the numbers of cells that had adhered to each sporocyst were scored. This was accomplished by examination of at least five discrete sites of the well of the 24-well plate with > 50 sporocysts of each group. The cell adhesion index (CAI) were scored from 1 to 4, with a score of 1 indicating few or no adherent cells and a score of 4 indicating that cells or clumps of cells covered more than half the tegumental surface of the sporocyst, as defined in earlier reports [26] (Fig. 3a). Cells from mock-transfected control mostly adhered in clumps or singly to the surface of the parasite (representative images in the upper panels of Fig. 3b), with CAI values that ranged from 2 to 4. By contrast, fewer cells adhered to the surface of the sporocysts in the Δ*Bg*AIF-Bge group (representative images, lower panels in Fig. 3B), with CAI values ranging from 2 to 3. Only ~ 20% of the Δ*Bg*AIF-Bge cells adhered to the surface of the sporocyst and most of the cells retained remained spread singly on the surface of the well of tissue culture plate (Fig. 3b). More specifically, the

mean CAI values ascertained from the seven biological replicates (≥ 50 parasites in each replicate (> 400 parasites scored), mean 2.66 ± 0.10, range, 2.53 to 2.78 in the mock-treated, transfection control group was significantly higher than the Δ*Bg*AIF group, mean. 2.25 ± 0.22, range, 2.08 to 2.55 (Fig. 3c) ($P \leq 0.01$, unpaired *t*-test). Morphological changes were not apparent among the Δ*Bg*AIF-Bge cells and the control group cells.

Discussion

This report describes a novel use of programmed genome editing by the CRISPR/Cas9 approach in the embryonic cell line from the gastropod snail, *B. glabrata*, an intermediate host snail of the human blood fluke, *S. mansoni.* The Bge cell line is an informative tool in investigation of snail-schistosome, host-parasite interactions. A key attribute of the Bge cell is its hemocyte-like phenotype, given the central role of the snail hemocyte in innate and cellular immunity. The allograft inflammatory factor 1 (AIF) is a conserved calcium-binding protein typically expressed in phagocytic and granular leukocytes and is a marker of macrophage activation [38, 41, 46, 61–64]. An orthologue, termed *Bg*AIF, is highly expressed in isolates of *B. glabrata* that are resistant to infection with *S. mansoni* and it has been suggested that this gene may be linked to hemocyte activation [8, 9]. Here, we targeted the *AIF* gene of *B. glabrata* using programmed gene knockout to further characterize its role in the intermediate host- schistosome interaction. We constructed a plasmid vector encoding the CRISPR/Cas9 nuclease and a guide RNA targeting exon 4 of *Bg*AIF gene and the Cas9 nuclease from *Streptococcus pyogenes*, and transfected Bge cells with the gene-editing construct by square wave electroporation. Transcript levels of *Bg*AIF were significantly reduced by up to 73% following transformation. In parallel, sequence reads of amplicons spanning the locus targeted for programmed gene knock-out revealed on-target mutation on the *Bg*AIF gene, that had been repaired by non-homologous end joining leading to gene-inactivating insertions and deletions. In addition, the adherence of gene-edited Bge cells to sporocysts was significantly impeded in comparison to control cells, as ascertained using a semi-quantitative, cell adherence index.

The *B. glabrata* internal defense system comprises hemocytes and soluble proteins found in the hemolymph, among them the *Bg*AIF [65–67]. The response of resistant mollusks is given by the adherence and encapsulation of sporocysts by hemocytes, leading to the parasite destruction [68]. The AIF-1 was demonstrated to be a pro-inflammatory cytokine that regulates immune-related genes of the oyster *Crassostrea ariakensis* [44]. Also, in the leech *Hirudo medicinalis*, *Hm*AIF-1, in addition to being involved in the innate immune response, like in other species, promotes macrophage-like migration by a chemotactic activity [41]. The adherence of *Bg*AIF gene-edited Bge cells to sporocysts was significantly impeded in comparison to control cells, as ascertained using a semi-quantitative cell adherence index. These cells, albeit in a low percentage, are less responsive to the *S. mansoni* parasite. These data suggest that, in the presence of *S. mansoni*, the Bge cells need to secrete *Bg*AIF for activating the recruitment of more Bge cells. Thus, the *Bg*AIF protein appears to play a role in cell recognition, migration, and/or adhesion, and it is, in some way, participating in the *B. glabrata* early immune response to the parasite. The AIF gene is highly conserved in several invertebrate and vertebrate species such as sponge, sea bream, rat, pig, and humans, being important in different organisms and probably performing a similar

functional role in the immune system by macrophage activation and migration [69]. In humans, the *Hm*AIF1 is an NF-κB pathway regulator, a pathway that comprises a family of evolutionarily conserved proteins, important to the immune system by participating in the expression of other proteins related to the immune system [70, 71]. Although additional experiments are needed to check the regulation of these pathways in *B. glabrata*, after the pathogen invasion, the *Bg*AIF possibly acts throughout the activation of the NF-κB pathway, which can lead to the recruitment of hemocytes and consequent pathogen elimination [70, 72].

These findings also confirmed the tractability of transfection of Bge cells by electroporation with the genome-editing construct, pCas-*Bg*AIFx4, and that the CMV promoter drove transcription of Cas9 in this snail species. Whereas transformation by plasmid DNA of Bge cells by square wave electroporation appears to be novel, Bge cells have been transformed in earlier reports using DNA complexed with cationic lipid-based transfection reagents and with polyethyleneimine [23] However, there are limitations to our study. Thus far we were unable to enrich the transfected cells from wild type cells, thus future studies using a drug selectable marker may address this impediment. Moreover, other approaches to deliver the CRISPR/Cas gene-editing cargo can be tried including repeated inoculation with ribonuclear protein complexes [73], titration of the transfection chemicals [74], titration of electroporation parameters [75], and/or transduction by lentiviral virions encoding the gRNA and *S. pyogenes* Cas9 nuclease as we have demonstrated with eggs *of S. mansoni* [55].

To conclude, here we provide a demonstration of gene editing in a cell line from a medically important taxon of freshwater gastropods that are vectors for the transmission of schistosomiasis. Moreover, we show the functional role of a *B. glabrata* allograft inflammatory factor in the migration/recognition of *S. mansoni* sporocysts *in vitro*. Furthermore, the demonstration of the activity of CRISPR/Cas9 gene editing in Bge cells suggests that genome editing in the germline and somatic tissues of intact *B. glabrata* snails will also be functional. Functional genomics using CRISPR/Cas-based genome editing in schistosomes and other trematodes responsible for major neglected tropical diseases has been reported [54, 55]. Accordingly, the establishment of a functional genomic protocols involving programmed gene editing to address fundamental questions in this host-parasite relationship using genetically modified snails and schistosomes now seems to be feasible.

Declarations

Acknowledgments

We thank Dr. Mathilde Knight for informative discussions on the snail-schistosome immunobiology and Dr. Margaret Mentink-Kane for support with the Bge cell line. Bge cells were provided by the NIAID Schistosomiasis Resource Center of the Biomedical Research Institute, Rockville, Maryland through NIH-NIAID contract HHSN272201000005I for distribution through BEI Resources. This work was supported by the Coordenação de Aperfeiçoamento de Pessoal de Nível Superior (CAPES) - finance code 001, Productivity fellowship from Conselho Nacional de Desenvolvimento Científico e Tecnológico (CNPq)

granted to MMM (302518/2018-5) and RLQ (308869/2017-6) and Fapemig (APQ-01766-15), Brazil, and the Wellcome Trust Strategic Award no. 107475/Z/15/Z, Functional Genomics Flatworms Initiative (FUGI) (Hoffmann, K.H., principal investigator, Brindley, P.J., co-investigator).

References

1. Webster JP, Davies CM. Coevolution and compatibility in the snail-schistosome system. Parasitology. 2001;123(Suppl):41–56.
2. El-Ansary A, Al-Daihan S. Important aspects of *Biomphalaria* snail-schistosome interactions as targets for antischistosome drug. Med Sci Monit. 2006;12(12):RA282–292.
3. Richards CS, Shade PC. The genetic variation of compatibility in *Biomphalaria glabrata* and *Schistosoma mansoni*. J Parasitol. 1987;73(6):1146–51.
4. Knight M, Miller A, Liu Y, Scaria P, Woodle M, Ittiprasert W. Polyethyleneimine (PEI) mediated siRNA gene silencing in the *Schistosoma mansoni* snail host, *Biomphalaria glabrata*. PLoS Negl Trop Dis. 2011;5(7):e1212.
5. Jannotti-Passos LK, Andrade HM, Caldeira RL, Romanha AJ, Murta SM, Chapeaurouge DA, Perales J, Coelho PM, Carvalho OS. Proteome analysis of the cardiac and pericardial tissue of *Biomphalaria tenagophila* populations susceptible and resistant to *Schistosoma mansoni* infection. Acta Trop. 2008;105(3):229–34.
6. Hanington PC, Lun CM, Adema CM, Loker ES. Time series analysis of the transcriptional responses of *Biomphalaria glabrata* throughout the course of intramolluscan development of *Schistosoma mansoni* and *Echinostoma paraensei*. Int J Parasitol. 2010;40(7):819–31.
7. Pila EA, Sullivan JT, Wu XZ, Fang J, Rudko SP, Gordy MA, Hanington PC. Haematopoiesis in molluscs: A review of haemocyte development and function in gastropods, cephalopods and bivalves. Dev Comp Immunol. 2016;58:119–28.
8. Lockyer AE, Emery AM, Kane RA, Walker AJ, Mayer CD, Mitta G, Coustau C, Adema CM, Hanelt B, Rollinson D, et al. Early differential gene expression in haemocytes from resistant and susceptible *Biomphalaria glabrata* strains in response to *Schistosoma mansoni*. PLoS One. 2012;7(12):e51102.
9. Larson MK, Bender RC, Bayne CJ. Resistance of *Biomphalaria glabrata* 13-16-R1 snails to *Schistosoma mansoni* PR1 is a function of haemocyte abundance and constitutive levels of specific transcripts in haemocytes. Int J Parasitol. 2014;44(6):343–53.
10. Pinaud S, Portela J, Duval D, Nowacki FC, Olive MA, Allienne JF, Galinier R, Dheilly NM, Kieffer-Jaquinod S, Mitta G, et al. A Shift from Cellular to Humoral Responses Contributes to Innate Immune Memory in the Vector Snail *Biomphalaria glabrata*. PLoS Pathog. 2016;12(1):e1005361.
11. Barbosa L, Caldeira RL, Carvalho OS, Vidigal TH, Jannotti-Passos LK, Coelho PM. Resistance to *Schistosoma mansoni* by transplantation of APO *Biomphalaria tenagophila*. Parasite Immunol. 2006;28(5):209–12.

12. Adema CM, Loker ES. Digenean-gastropod host associations inform on aspects of specific immunity in snails. Dev Comp Immunol. 2015;48(2):275–83.
13. Coustau C, Gourbal B, Duval D, Yoshino TP, Adema CM, Mitta G. Advances in gastropod immunity from the study of the interaction between the snail *Biomphalaria glabrata* and its parasites: A review of research progress over the last decade. Fish Shellfish Immunol. 2015;46(1):5–16.
14. Mitta G, Adema CM, Gourbal B, Loker ES, Theron A. Compatibility polymorphism in snail/schistosome interactions: From field to theory to molecular mechanisms. Dev Comp Immunol. 2012;37(1):1–8.
15. Mitta G, Gourbal B, Grunau C, Knight M, Bridger JM, Theron A. The Compatibility Between *Biomphalaria glabrata* Snails and *Schistosoma mansoni*: An Increasingly Complex Puzzle. Adv Parasitol. 2017;97:111–45.
16. Pila EA, Li H, Hambrook JR, Wu X, Hanington PC. Schistosomiasis from a Snail's Perspective: Advances in Snail Immunity. Trends Parasitol. 2017;33(11):845–57.
17. Famakinde DO. Molecular context of *Schistosoma mansoni* transmission in the molluscan environments: A mini-review. Acta Trop. 2017;176:98–104.
18. Knight M, Arican-Goktas HD, Ittiprasert W, Odoemelam EC, Miller AN, Bridger JM. Schistosomes and snails: a molecular encounter. Front Genet. 2014;5:230.
19. Yescott RE, Hansen E. Effect of manganese on *Biomphalaria glabrata* infected with *Schistosoma mansoni*. J Invertebr Pathol. 1976;28(3):315–20.
20. Laursen JR, Yoshino TP. *Biomphalaria glabrata* embryonic (Bge) cell line supports *in vitro* miracidial transformation and early larval development of the deer liver fluke, *Fascioloides magna*. Parasitology. 1999;118(Pt 2):187–94.
21. Wheeler NJ, Dinguirard N, Marquez J, Gonzalez A, Zamanian M, Yoshino TP, Castillo MG. Correction to: Sequence and structural variation in the genome of the *Biomphalaria glabrata* embryonic (Bge) cell line. Parasit Vectors. 2018;11(1):566.
22. Wheeler NJ, Dinguirard N, Marquez J, Gonzalez A, Zamanian M, Yoshino TP, Castillo MG. Sequence and structural variation in the genome of the *Biomphalaria glabrata* embryonic (Bge) cell line. Parasit Vectors. 2018;11(1):496.
23. Rinaldi G, Yan H, Nacif-Pimenta R, Matchimakul P, Bridger J, Mann VH, Smout MJ, Brindley PJ, Knight M. Cytometric analysis, genetic manipulation and antibiotic selection of the snail embryonic cell line Bge from *Biomphalaria glabrata*, the intermediate host of *Schistosoma mansoni*. Int J Parasitol. 2015;45(8):527–35.
24. Odoemelam E, Raghavan N, Miller A, Bridger JM, Knight M. Revised karyotyping and gene mapping of the *Biomphalaria glabrata* embryonic (Bge) cell line. Int J Parasitol. 2009;39(6):675–81.
25. Vermeire JJ, Boyle JP, Yoshino TP. Differential gene expression and the effects of *Biomphalaria glabrata* embryonic (Bge) cell factors during larval *Schistosoma mansoni* development. Mol Biochem Parasitol. 2004;135(1):153–7.

26. Castillo MG, Yoshino TP. Carbohydrate inhibition of *Biomphalaria glabrata* embryonic (Bge) cell adhesion to primary sporocysts of *Schistosoma mansoni*. Parasitology. 2002;125(Pt 6):513–25.
27. Humphries JE, Elizondo L, Yoshino TP. Protein kinase C regulation of cell spreading in the molluscan *Biomphalaria glabrata* embryonic (Bge) cell line. Biochim Biophys Acta. 2001;1540(3):243–52.
28. Yoshino TP, Laursen JR. Production of *Schistosoma mansoni* daughter sporocysts from mother sporocysts maintained in synxenic culture with *Biomphalaria glabrata* embryonic (Bge) cells. J Parasitol. 1995;81(5):714–22.
29. Adema CM, Hillier LW, Jones CS, Loker ES, Knight M, Minx P, Oliveira G, Raghavan N, Shedlock A, do Amaral LR, et al. Whole genome analysis of a schistosomiasis-transmitting freshwater snail. Nat Commun. 2017;8:15451.
30. Dheilly NM, Duval D, Mouahid G, Emans R, Allienne JF, Galinier R, Genthon C, Dubois E, Du Pasquier L, Adema CM, et al. A family of variable immunoglobulin and lectin domain containing molecules in the snail *Biomphalaria glabrata*. Dev Comp Immunol. 2015;48(1):234–43.
31. Zhang SM, Loker ES. Representation of an immune responsive gene family encoding fibrinogen-related proteins in the freshwater mollusc *Biomphalaria glabrata*, an intermediate host for *Schistosoma mansoni*. Gene. 2004;341:255–66.
32. Portet A, Pinaud S, Tetreau G, Galinier R, Cosseau C, Duval D, Grunau C, Mitta G, Gourbal B. Integrated multi-omic analyses in *Biomphalaria-Schistosoma* dialogue reveal the immunobiological significance of FREP-SmPoMuc interaction. Dev Comp Immunol. 2017;75:16–27.
33. Hanington PC, Zhang SM. The primary role of fibrinogen-related proteins in invertebrates is defense, not coagulation. J Innate Immun. 2011;3(1):17–27.
34. Adema CM. Fibrinogen-Related Proteins (FREPs) in Mollusks. Results Probl Cell Differ. 2015;57:111–29.
35. Gordy MA, Pila EA, Hanington PC. The role of fibrinogen-related proteins in the gastropod immune response. Fish Shellfish Immunol. 2015;46(1):39–49.
36. Baranzini N, Monti L, Vanotti M, Orlandi VT, Bolognese F, Scaldaferri D, Girardello R, Tettamanti G, de Eguileor M, Vizioli J, et al. AIF-1 and RNASET2 Play Complementary Roles in the Innate Immune Response of Medicinal Leech. J Innate Immun. 2019;11(2):150–67.
37. Ai XL, Yao F, Wang XJ, Duan DB, Li K, Hu ZY, Yin G, Wang M, Wu BY. [Role of allograft inflammatory factor-1 in regulating the proliferation, migration and apoptosis of colorectal cancer cells]. Nan Fang Yi Ke Da Xue Xue Bao. 2018;38(5):511–9.
38. Zhang Y, Li J, Yu F, He X, Yu Z. Allograft inflammatory factor-1 stimulates hemocyte immune activation by enhancing phagocytosis and expression of inflammatory cytokines in *Crassostrea gigas*. Fish Shellfish Immunol. 2013;34(5):1071–7.
39. Jia J, Cai Y, Wang R, Fu K, Zhao YF. Overexpression of allograft inflammatory factor-1 promotes the proliferation and migration of human endothelial cells (HUV-EC-C) probably by up-regulation of basic fibroblast growth factor. Pediatr Res. 2010;67(1):29–34.

40. Autieri MV, Carbone CM. Overexpression of allograft inflammatory factor-1 promotes proliferation of vascular smooth muscle cells by cell cycle deregulation. Arterioscler Thromb Vasc Biol. 2001;21(9):1421–6.
41. Schorn T, Drago F, Tettamanti G, Valvassori R, de Eguileor M, Vizioli J, Grimaldi A. Homolog of allograft inflammatory factor-1 induces macrophage migration during innate immune response in leech. Cell Tissue Res. 2015;359(3):853–64.
42. Martin-Gomez L, Villalba A, Carballal MJ, Abollo E. Molecular characterisation of TNF, AIF, dermatopontin and VAMP genes of the flat oyster Ostrea edulis and analysis of their modulation by diseases. Gene. 2014;533(1):208–17.
43. Li J, Chen J, Zhang Y, Yu Z. Expression of allograft inflammatory factor-1 (AIF-1) in response to bacterial challenge and tissue injury in the pearl oyster, *Pinctada martensii*. Fish Shellfish Immunol. 2013;34(1):365–71.
44. Xu T, Xie J, Zhu B, Liu X, Wu X. allograft inflammatory factor 1 functions as a pro-inflammatory cytokine in the oyster, *Crassostrea ariakensis*. PLoS One. 2014;9(4):e95859.
45. Chen QR, Guan F, Song SM, Jin JK, Lei DS, Chen CM, Lei JH, Chen ZW, Niu AO. Allograft inflammatory factor-1 alleviates liver disease of BALB/c mice infected with *Schistosoma japonicum*. Parasitol Res. 2014;113(7):2629–39.
46. Chen QR, Guan F, Yan DJ, Lei DS, Fu L, Xia HS, Zhu YH, Chen ZW, Niu AO. The dynamic expression of allograft inflammatory factor-1 in hepatic tissues and splenic cells of BALB/c mice with *Schistosoma japonicum* infection. Tissue Antigens. 2012;79(1):33–41.
47. Yu H, Li H, Li Q, Xu R, Yue C, Du S. Targeted Gene Disruption in Pacific Oyster Based on CRISPR/Cas9 Ribonucleoprotein Complexes. Mar Biotechnol (NY). 2019;21(3):301–9.
48. Perry KJ, Henry JQ. CRISPR/Cas9-mediated genome modification in the mollusc, *Crepidula fornicata*. Genesis. 2015;53(2):237–44.
49. Abe M, Kuroda R. The development of CRISPR for a mollusc establishes the formin Lsdia1 as the long-sought gene for snail dextral/sinistral coiling. *Development* 2019, 146(9).
50. Labun K, Montague TG, Gagnon JA, Thyme SB, Valen E. CHOPCHOP v2: a web tool for the next generation of CRISPR genome engineering. Nucleic Acids Res. 2016;44(W1):W272–6.
51. Labun K, Montague TG, Krause M, Torres Cleuren YN, Tjeldnes H, Valen E. CHOPCHOP v3: expanding the CRISPR web toolbox beyond genome editing. Nucleic Acids Res. 2019;47(W1):W171–4.
52. Montague TG, Cruz JM, Gagnon JA, Church GM, Valen E. CHOPCHOP: a CRISPR/Cas9 and TALEN web tool for genome editing. *Nucleic Acids Res* 2014, 42(Web Server issue):W401-407.
53. Knight M, Ittiprasert W, Odoemelam EC, Adema CM, Miller A, Raghavan N, Bridger JM. Non-random organization of the *Biomphalaria glabrata* genome in interphase Bge cells and the spatial repositioning of activated genes in cells co-cultured with *Schistosoma mansoni*. Int J Parasitol. 2011;41(1):61–70.
54. Arunsan P, Ittiprasert W, Smout MJ, Cochran CJ, Mann VH, Chaiyadet S, Karinshak SE, Sripa B, Young ND, Sotillo J, et al: Programmed knockout mutation of liver fluke granulin attenuates virulence of

infection-induced hepatobiliary morbidity. *Elife* 2019, 8.

55. Ittiprasert W, Mann VH, Karinshak SE, Coghlan A, Rinaldi G, Sankaranarayanan G, Chaidee A, Tanno T, Kumkhaek C, Prangtaworn P, et al: Programmed genome editing of the omega-1 ribonuclease of the blood fluke, *Schistosoma mansoni*. *Elife* 2019, 8.
56. Brinkman EK, Kousholt AN, Harmsen T, Leemans C, Chen T, Jonkers J, van Steensel B. Easy quantification of template-directed CRISPR/Cas9 editing. Nucleic Acids Res. 2018;46(10):e58.
57. Brinkman EK, van Steensel B. Rapid Quantitative Evaluation of CRISPR Genome Editing by TIDE and TIDER. Methods Mol Biol. 2019;1961:29–44.
58. Hsiau T, Maures T, Waite K, Yang J, Kelso R, Holden K, Stoner R: Inference of CRISPR edits from Sanger Trace Data. *bioRxiv* 2018.
59. Livak KJ, Schmittgen TD. Analysis of relative gene expression data using real-time quantitative PCR and the 2(-Delta Delta C(T)) Method. Methods. 2001;25(4):402–8.
60. Symington LS, Gautier J. Double-strand break end resection and repair pathway choice. Annu Rev Genet. 2011;45:247–71.
61. Donovan KM, Leidinger MR, McQuillen LP, Goeken JA, Hogan CM, Harwani SC, Flaherty HA, Meyerholz DK. Allograft Inflammatory Factor 1 as an Immunohistochemical Marker for Macrophages in Multiple Tissues and Laboratory Animal Species. Comp Med. 2018;68(5):341–8.
62. De Zoysa M, Nikapitiya C, Kim Y, Oh C, Kang DH, Whang I, Kim SJ, Lee JS, Choi CY, Lee J. Allograft inflammatory factor-1 in disk abalone (*Haliotis discus discus*): molecular cloning, transcriptional regulation against immune challenge and tissue injury. Fish Shellfish Immunol. 2010;29(2):319–26.
63. Li Q, Bai Z, Zhao L, Li J. Characterization of allograft inflammatory factor-1 in *Hyriopsis cumingii* and its expression in response to immune challenge and pearl sac formation. Fish Shellfish Immunol. 2016;59:241–9.
64. Liu G, Ma H, Jiang L, Zhao Y. Allograft inflammatory factor-1 and its immune regulation. Autoimmunity. 2007;40(2):95–102.
65. van der Knaap WP, Loker ES. Immune mechanisms in trematode-snail interactions. Parasitol Today. 1990;6(6):175–82.
66. Vergote D, Bouchut A, Sautiere PE, Roger E, Galinier R, Rognon A, Coustau C, Salzet M, Mitta G. Characterisation of proteins differentially present in the plasma of *Biomphalaria glabrata* susceptible or resistant to *Echinostoma caproni*. Int J Parasitol. 2005;35(2):215–24.
67. Negrao-Correa D, Mattos AC, Pereira CA, Martins-Souza RL, Coelho PM. Interaction of *Schistosoma mansoni* Sporocysts and Hemocytes of *Biomphalaria*. J Parasitol Res. 2012;2012:743920.
68. Guaraldo AM, Magalhaes LA, Rangel Hde A, Pareja G. [Evolution of spopocysts of *Schistosoma mansoni* Sambon 1907 in *Biomphalaria glabrata* (Say 1818) and *Biomphalaria tenagophila* (d'Orbigny 1835)]. Rev Saude Publica. 1981;15(4):436–48.
69. Watano K, Iwabuchi K, Fujii S, Ishimori N, Mitsuhashi S, Ato M, Kitabatake A, Onoe K. Allograft inflammatory factor-1 augments production of interleukin-6, -10 and – 12 by a mouse macrophage

line. Immunology. 2001;104(3):307–16.

70. Symeonidou I, Kourelis A, Frydas I, Karagouni E, Anogeianaki A, Hatzistilianou M, Frydas S. Modulation of NF-kappaBeta signalling pathways by parasites. J Biol Regul Homeost Agents. 2010;24(4):471–9.
71. Tato CM, Hunter CA. Host-pathogen interactions: subversion and utilization of the NF-kappa B pathway during infection. Infect Immun. 2002;70(7):3311–7.
72. Egana-Gorrono L, Chinnasamy P, Casimiro I, Almonte VM, Parikh D, Oliveira-Paula GH, Jayakumar S, Law C, Riascos-Bernal DF, Sibinga NES. Allograft inflammatory factor-1 supports macrophage survival and efferocytosis and limits necrosis in atherosclerotic plaques. Atherosclerosis. 2019;289:184–94.
73. Lin S, Staahl BT, Alla RK, Doudna JA. Enhanced homology-directed human genome engineering by controlled timing of CRISPR/Cas9 delivery. Elife. 2014;3:e04766.
74. Lino CA, Harper JC, Carney JP, Timlin JA. Delivering CRISPR: a review of the challenges and approaches. Drug Deliv. 2018;25(1):1234–57.
75. Fajrial AK, He QQ, Wirusanti NI, Slansky JE, Ding X. A review of emerging physical transfection methods for CRISPR/Cas9-mediated gene editing. Theranostics. 2020;10(12):5532–49.

Figures

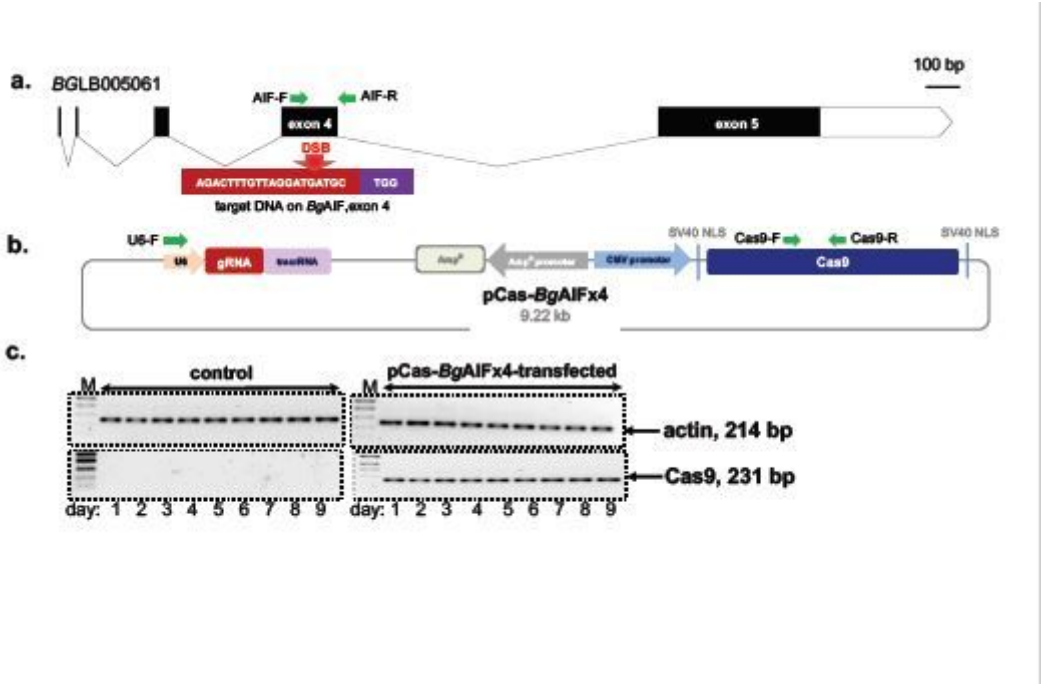

Figure 1

Schematic diagram of BgAIF gene structure, CRISPR/Cas9 vector and expression in Bge cell. Panel a.Gene structure of B. glabrata allograft inflammatory factor (BgAIF), accession number BGLB005061 and gene editing target locus (red box) on exon 4. BgAIF gene composed of 5 exons and 4 introns. The

green arrows indicate the location of primers flanking expected DSBs which were used in PCR to generate the on-target amplicon for INDELs estimation.Panel b. Map of the pCas-BgAIFx4 vector which includes the Pol III-dependent mammalian U6 gene promoter (red arrow) to drive transcription of the guide RNA targeting exon 4 of BgAIF gene (red arrow) and the CMV promoter to drive expression of the S. pyogenes Cas9 nuclease (blue arrow). Primer pairs specific for the guide RNA and for Cas9 are indicated (green arrows).Panel c.Expression ofCas9 and of BgActin (as the reference gene) transcripts as established by semi-quantitative RT-PCR in pCas-BgAIF-transfected (right) and control (left) Bge cells from days one to nine following transfection. The amplicons of the expected sizes are as indicated: 23 bp for Cas9 and 214 bp for BgActin. All RNA samples were positive for the BgActin reference gene; the 214 bp band.

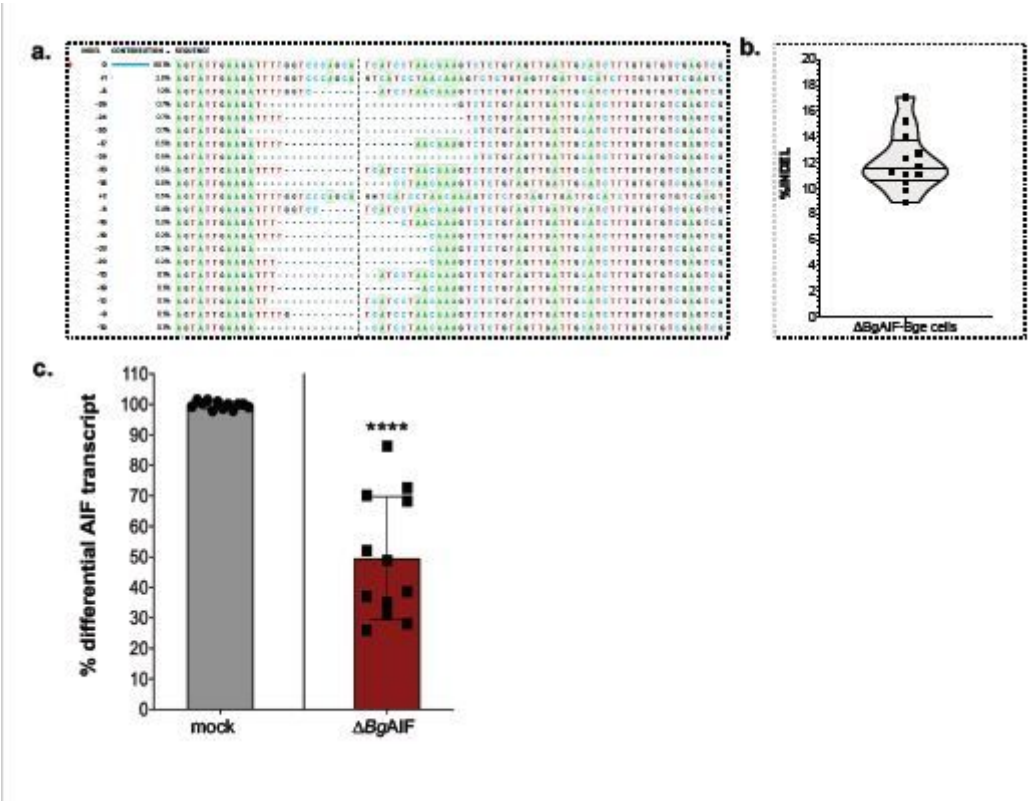

Figure 2

Establishment of BgAIF-knockout lines of Bge cells. Panela. Representative examples of frequent gene insertions-deletions (1-2 bp insertions and 8-30 bp deletions, straddling the programmed CRISPR/Cas9-induced double-stranded break in exon 4, as determined by ICE software-based analysis. Panel b. TIDE algorithm-based violin plot of insertion-deletion percentages (%INDEL) computed using the amplicon sequence traces from the 12 biological replicates of pCas-BgAIF-transfected Bge cell populations. Panel c. Reduction of BgAIF transcription by about 50% following programmed genome editing of Bge cells (ΔBgAIF-Bge) in comparison to control Bge cells. Mean transcript reduction, 49.55± 20.22 (S.D.) percent, $P \leq 0.0001$ (****), n =12 (unpaired Student's t-test).

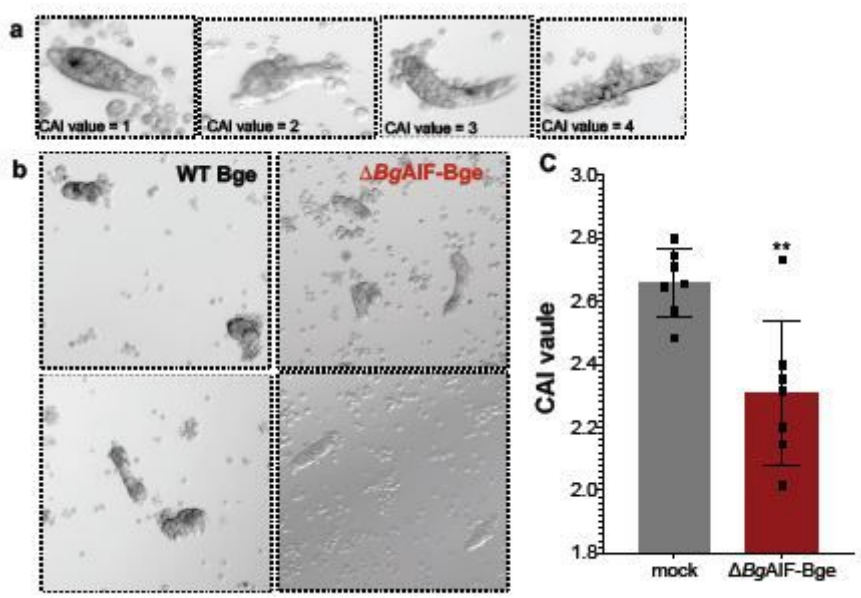

Figure 3

Programmed knockout of BgAIF in Bge cells caused reduced adherence to primary sporocysts. Panel a. Representative micrographs of primary sporocysts co-cultured with Bge cells in our laboratory to profile the semi-quantitative scoring of the cell adhesion index (CAI); CAI value = 1; no cells adhering to the surface of the sporocyst; value = 2; ≤10 cells adhering to the sporocyst; value = 3; > 10 cells < half of the sporocyst surface covered by cells or clumps of cells; value = 4; > half the sporocyst surface covered by Bge cells. Panel b. Representative micrographs indicatethe reduced levels of ΔBgAIF-Bge cells adherence(right panel) in comparison to control, mock-transfected Bge cells (left panel) to the co-cultured sporocysts. Panel c. Bar chart to present the CAI values from control (mock-transfected) ΔBgAIF-Bge cells during co-culture with primary sporocysts at a co-culture ratio of one sporocyst to 100 Bge cells; CAI value = 2.66±0.10, mean ±SD (476 sporocysts in total scored) for the mock-transfected Bge and 2.31±0.23 for the ΔBgAIF-Bge cells (424 sporocysts in total scored); P = 0.0033, unpaired Student's t test; n =7 biological replicates.